RSC Advances

ROYAL SOCIETY OF CHEMISTRY

www.rsc.org/advances

Thermo-mechanical and dielectric properties of graphene reinforced caprolactam cardanol based benzoxazine-epoxy nanocomposites

K. Sethuraman[a] and M. Alagar[a]*

[a] Polymer Composite Lab, Department of Chemical Engineering, Anna University, Chennai-600 025, India

[a)] Tel.: + 91 44 2235 9164; Fax: +91 44 2235 9164; Electronic mail: mkalagar@yahoo.com and muthukaruppanalagar@gmail.com

Abstract

In the present work a new type of benzoxazine was synthesized using caproamine with cardanol and their molecular structure was characterized by FTIR and NMR spectroscopy. The graphene reinforced epoxy-polybenzoxazine nanocomposites was prepared by incorporating varying weight percentages of graphene and benzoxazine to epoxy resin. Data obtained from mechanical study infer the significant improvement in the values of tensile strength, impact strength and flexural strength of the composites reinforced with different weight percentages of benzoxazine and graphene. The values of dielectric constant of composite samples are appreciably enhanced and are higher than that of neat epoxy matrix. Data from SEM, TEM and XRD ascertain the existence of homogeneous distribution of graphene in the composites. Data obtained from thermal, mechanical, dielectric and surface free energy studies infer that 20 wt% Bz-g reinforced composites possesses better properties than those of neat epoxy matrix and other weight percentages of composites.

Key Words: Cardanol, caprolactam, benzoxazine, impact strength, dielectric constant.

Introduction

Polybenzoxazines are a class of thermosetting phenolic resins obtained from benzoxazine through ring opening polymerization of oxirane ring in the absence of a catalyst, releasing no byproducts. The Polybenzoxazine have many advantages like near-zero shrinkage upon polymerization, low water absorption, high char yield, excellent dimensional stability, flame retardance, stable dielectric constant, and low surface free energy. Although, polybenzoxazines offer a variety of advantages, neat

polybenzoxazine-based polymers suffer a certain disadvantages too. The high temperature required for curing and the brittleness of the cured materials limit their potential applications. To properly address these issues and overcome the associated disadvantages, the most successful strategies are the preparation of monomers with suitable molecular structure and blending them with high performance polymer and suitable reinforcement[1].Caprolactam (CPL) is a cyclic amide of caproic acid and is widely used as precursor for synthetic polymer. Caprolactam possesses better combination of thermo mechanical properties suitable for the fabrication of polymer composites because of its flexible structure (-NH-CO-) formed during in situ reaction of cyclic aliphatic caprolactam with benzoxazine. Cardanol is a well known phenolic compound obtained as a renewable bio source. Polybenzoxazine developed using cardanol have received much research attention because they overcome many of the deficiencies commonly associated with conventional novolac and resol-type phenolic resins[2,3]. They have demonstrated various attractive properties including high thermal stability, high char yield, high glass transition temperature (Tg), near-zero volumetric change upon curing, good mechanical and dielectric properties, low water absorption, low flammability, and excellent solubility in common organic solvents. These characteristics make benzoxazine polymers become an excellent materials for high performance composites[4-7].

Thermosetting resins can be used as an efficient dielectric material in embedded capacitor technology if their electrical property is improved with suitable reinforcements[8]. Thermosetting polymers with metals and ceramics are widely used in capacitor technology, however their high density, poor processability and low adhesion strength restrict their use in lightweight aerospace applications[9]. If these materials are blended with light weight materials like capron and graphene it will be suitable for high performance light weight dielectric applications. Graphene exhibits fascinating electronic, thermal, and mechanical properties due to its unique structure and also possesses an ability to be dispersed in various polymer matrices make graphene become most suitable for the development of next-generation polymer hybrid nanocomposites[10-12]. Epoxy resins are well known industrial material used in the form of electronic encapsulants, electrical laminates, structural adhesives and composite materials. Like Polybenzoxazine, epoxy also exhibit an inherent brittle nature and poor crack resistance and limits its utility for high performance applications. Many attempts have been made to improve toughness, stiffness and strength of epoxy resins by blending with numerous chemical modifiers, reinforcements etc.[13-16] An improvement property of cardanol-epoxy composites and graphene–benzoxazine/epoxy nanocomposites developed for capacitor applications are also reported in the literature[17-19].

In the present work an attempt has been made to develop hybrid composite materials based on industrially potential and commercially competitive resin ie epoxy and benzoxazine with graphene reinforcement. The prime objective of the present work involves 1. Toughening of epoxy and benzoxazine resin, 2. The development of benzoxazine graphene reinforced epoxy composites, 3. To enhance thermo mechanical and dielectric behaviour to make them useful for efficient capacitive applications by reinforcing with graphene, 4. To utilize renewable resource cardanol biomaterial for synthesis of structurally modified benzoxazine suitable for toughening of epoxy resin, 5. To utilize resilient caprolactam to enhance thermo mechanical behaviour of hybrid composites. With those objectives in view the hybrid epoxy based composites reinforced with varying weight percentages of Bz-g were developed and characterized by different sophisticated analytical techniques and the data resulted are discussed and reported.

Experimental methods

Materials

Cardanol was obtained from Sathya Cashew products Chennai. Formaldehyde, N-methyl 2-pyrrolidone, sodium hydroxide, potassium permanganate, chloroform, and hydrazine hydrate were purchased from Merck and were used as received. Diglycidyl ether of bisphenol – A (DGEBA epoxy resin) (LY556) was utilized as matrix resin in the present study and it was received from Ciba-Geigy Ltd. Natural graphite was purchased from Active Carbon India Pvt. Ltd., India. Sulfuric acid (H_2SO_4, 95-98%) was purchased from Ranbaxy Chemicals, India. Hydrogen peroxide (H_2O_2) was purchased from SD Fine Chemicals, India. Sodium nitrate ($NaNO_3$), caprolactam, sodium hypo phosphate, dimethylformamide (DMF) and diphenyldiaminomethane (DDM) were purchased from SRL chemicals, Chennai.

Synthesis of N, N'-(4,4'-methylenebis (4,1-phenylene))bis(6-aminohexanamide)-(CPA)

CPA was synthesized as per modified procedure reported earlier by our research group[20]. In a 250 mL two necked round bottomed flask equipped with condenser, 100 mL of N-methyl pyrrolidone (NMP), 10g (0.0883 mol) of caprolactam, 7.8g (0.0442 mol) of 4, 4' methylenedianiline and 5mg of alkali hypo

phosphate catalyst were added. The mixture was allowed react at 100 ^{0}C for 24 h with efficient agitation to facilitate completion of reaction. The product was filtered by separation. (Yield 85%). (Scheme 1)

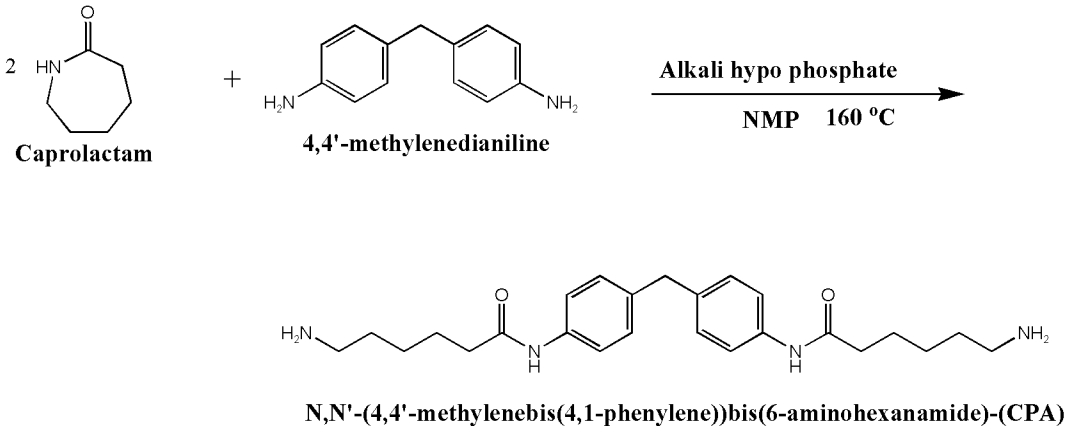

Scheme 1. Synthesis of CPA.

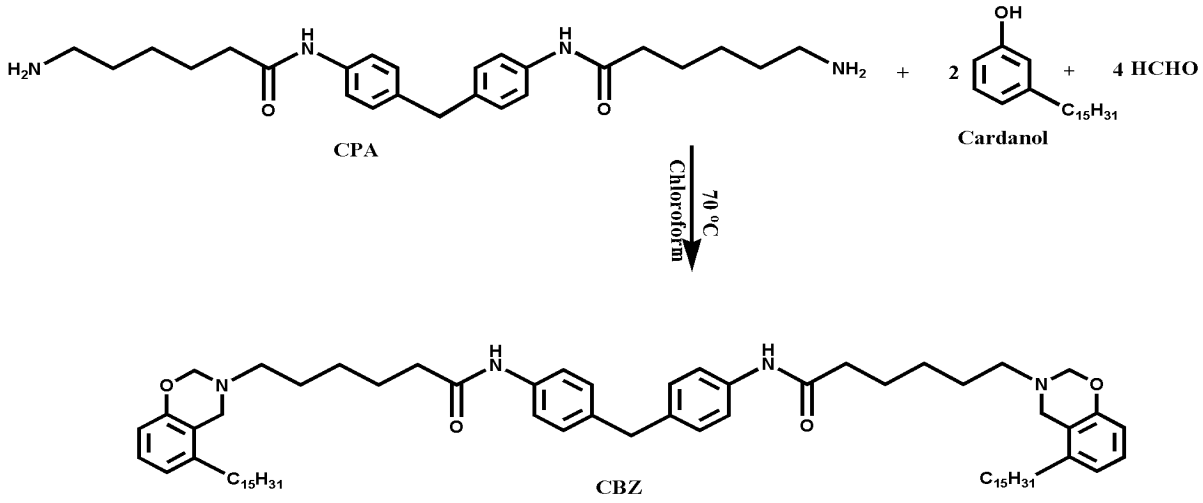

Scheme 2. Synthesis of CPA- cardanol benzoxazine (CBZ).

Synthesis of CPA- cardanol benzoxazine (CBZ)

To the CPA (5g, 0.011mol) in chloroform, formaldehyde (1.4g, 0.047mol) was added and stirred for 30 minutes at 0 ^{o}C. Subsequently, 7.42g of cardanol (0.023mol) was added to the reaction mixture and stirred for overnight at 70 ^{o}C. After the completion of reaction, the reaction mixture was extracted with

ethyl acetate and washed with 2N NaOH, water, brine and concentrated the organic layer to obtain the product.(Yield 95 %).(Scheme 2) and preserved for further use.

Synthesis of graphene

Graphene Oxide (GO) was prepared from natural graphite through modified Hummer's method[21]. About 1 g of graphite and 1.2 g of $NaNO_3$ were added to 69mL of concentrated H_2SO_4, and then 3 g of KMO_4 was gradually added with stirring and then the reaction mixture was heated at 35 ^{0}C for 6 h. In the next step, about 80mL distilled water was slowly added to the mixture, which was maintained at 60 ^{0}C for 30 min. Finally, 200mL distilled water and 6mL of 30 wt% H_2O_2 were added. The product was washed repeatedly with Ultra pristine Milli-Q water using centrifugation method until the homogeneous colloidal suspension was obtained. An aqueous suspension of exfoliated GO, with ~20 mg/mL was obtained by centrifugation. To the exfoliated GO 250 mL of water is added to get a homogeneous dispersion. This dispersion was sonicated using an ultrasonicator. Hydrazine hydrate (3.5ml. 0.1 mol) was then added and the solution was heated in an oil bath at 100 ^{0}C under a water-cooled condenser for 24 h over which the reduced GO gradually precipitated out as a black solid. The product was isolated by filtration and washed with water and then with methanol and dried in hot air oven and preserved for further use.

Development of benzoxazine-graphene/epoxy nanocomposites

The benzoxazine-graphene/ epoxy nanocomposites was developed by following method.The purified benzoxazine monomer (0.2 mol) and 1 wt% of graphene was dispersed in 100 mL of DMF and taken in a round bottomed flask and refluxed at 120 ^{0}C at 24 h. After cooling to room temperature, the above product was filtered and used as the precursor for the composite preparation. The blend of benzoxazine-graphene (Bz-g) was added with varying percentages (5wt%, 10wt%, 15wt% and 20wt %) to epoxy resin. The stiochometric amount of DDM curative was added (Table 1) to epoxy resin and then cured at 140^{0}C for 1 h, 180^{0}C for 1 h, and post cured at 220^{0}C for 2 h.

Table 1. The composition material used sfor the development of neat epoxy and Bz-g/Ep nanocomposites.

Sample code	Epoxy resin (g)	Benzoxazine - graphene blend (g)	DDM (g)
Neat Epoxy	40	0	11.65
5wt% Bz-g/Ep	38	2	11.06
10wt% Bz-g/Ep	36	4	10.50
15wt% Bz-g/Ep	34	6	9.90
20wt% Bz-g/Ep	32	8	9.32

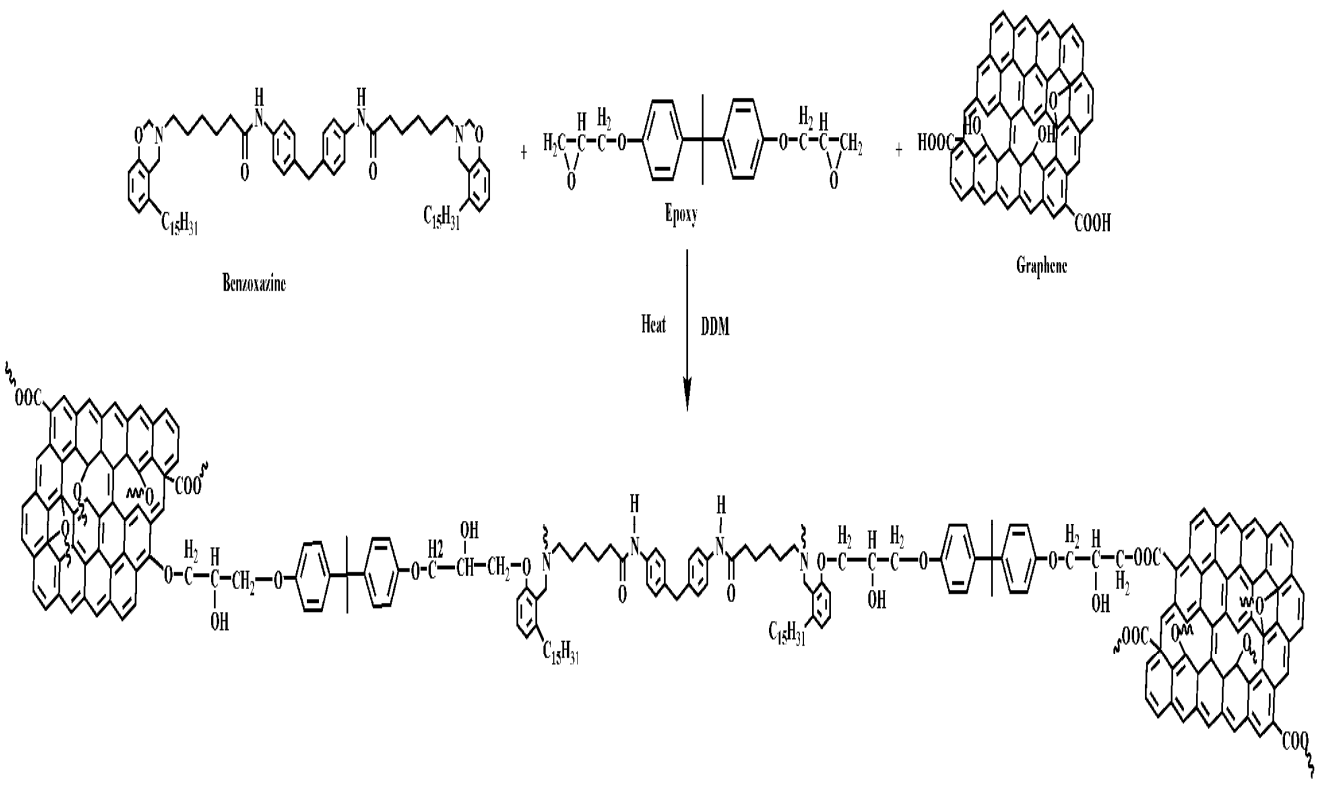

Scheme 3. Development of benxoxazine-grahene/ epoxy nanocomposites.

Characterization

Fourier-transform infrared (FTIR) spectra of KBr disks were obtained using a Bruker Tensor 27 FT-IR spectrophotometer. Proton nuclear magnetic resonance (^{1}H-NMR) and ^{13}C-NMR of the benzoxazine monomer were obtained from Bruker AV III FT-NMR spectrometer operating at a frequency of 500 MHz. The sample was dissolved in deuterated chloroform and tetramethylsilane was used as an internal standard. Thermogravimetric and differential scanning calorimetric analyses of the composites were carried out with a Exstar 6300 at a heating rate of 10 °C/min under nitrogen atmosphere.

Raman spectra were measured on a Lab RAM HR UV–VIS–NIR Raman Microscope from HORIBA Jobin–Yvon (633 nm laser source). The dielectric studies of the neat epoxy and Bz-g/Ep nanocomposites were determined using Broad band Dielectric Spectrometer (BDS), NOVOCONTROL Technologies GmbH & Co. (Model Concept 80) at 30ºC in the range of 1Hz to 1MHz.For dielectric measurement the samples were made as pellet and directly used.

The surface morphology of the fractured surface of the samples was examined using a scanning electron microscope (SEM; JEOL JSM Model 6360). A JEOL JEM-3010 analytical transmission electron microscope operating at 80 kV with a measured point-to-point resolution of 0.23 nm was used to characterize the phase morphology of the developed nanocomposites. TEM samples were prepared by dispersing powder sample of composites under sonication in ethanol and were mounted on carbon-coated Cu TEM grids and dried for 1 h at 70 ^{0}C to form a film of <100 nm. Contact angle measurements were carried out using 210 a Rame-hart Inc. goniometer (Succasunna, NJ, USA) with 5 ml of deionised water and diiodimethane (DIM).

X-ray diffraction patterns were recorded at room temperature, by monitoring the diffraction angle 2θ from 10 to 80˚ as the standard, on a Rich Seifert (Model 3000) X-ray powder diffractometer. The tensile strength was determined, using INSTRON (Model 6025 UK) as per ASTM D 3039 at 10 mm min^{-1} cross-head speed, using specimens with dimensions of 100 mm×25 mm ×3 mm. The flexural strength was measured by the INSTRON (Model 6025 UK) as per ASTM D 790, using specimens with dimensions of 100 mm ×10 mm × 3 mm at 10 mm min^{-1} cross-head speed. The un-notched Izod impact

strength of sample was studied as per ASTM D 256, using specimen dimensions of 65 mm × 10 mm × 3 mm.

Results and Discussion

FTIR Spectra

Figure 1a shows the FTIR spectra of caproamine (CPA). In the figure the peak appeared at 3347 cm^{-1} represents for N-H stretching vibration. Peaks appeared at 2931, 1670 and 1609 cm^{-1} represent for C=O amide, NH_2 deformation and aromatic C-N stretching respectively. Figure 1b presents the FT-IR spectrum of GO and graphite. The O–H stretching is appeared at 3300–3500 cm^{-1} as a broad peak, C=O and C-O stretching vibration occurs at 1717 cm^{-1} and 1204 cm^{-1} respectively[22] and confirm the formation of graphene oxide.

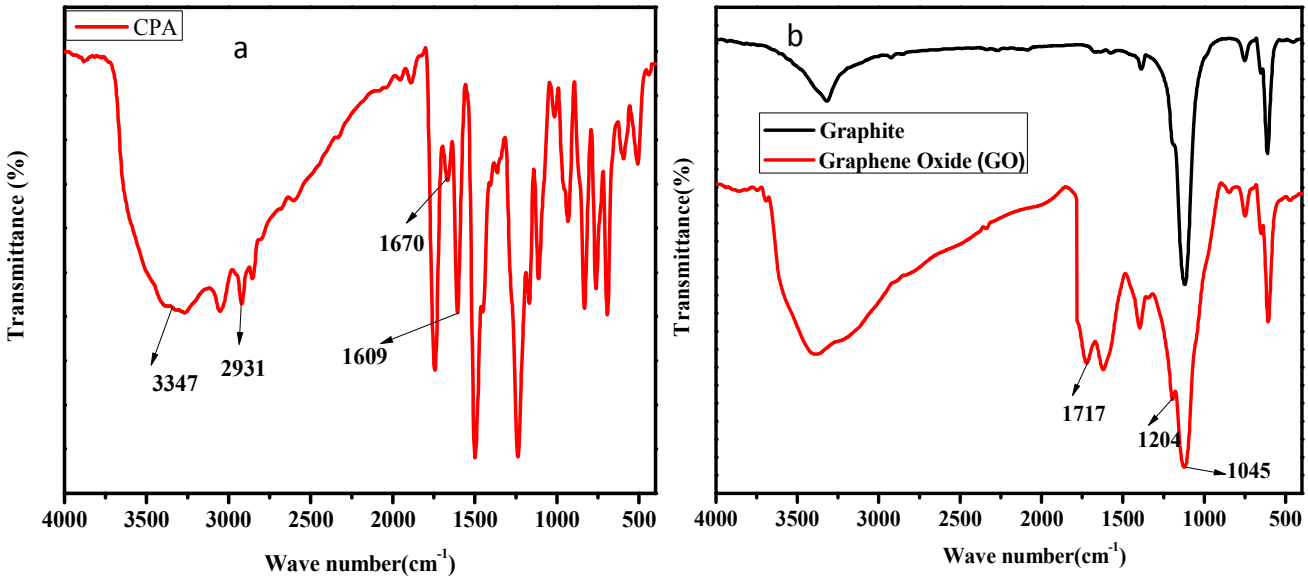

Figure 1. (a) FTIR spectra of CPA amine and (b) Graphite and Graphene oxide.

Figure 2a shows the FT-IR spectra of cardanol benzoxazine (CBZ). The peaks appeared at 1227 cm^{-1} and 1035 cm^{-1} represent asymmetric and symmetric stretching vibrations of C-O-C bond in the benzoxazine respectively. The appearance of new peak at 945 cm^{-1} corresponds to stretching vibration of C-O moiety from benzoxazine.

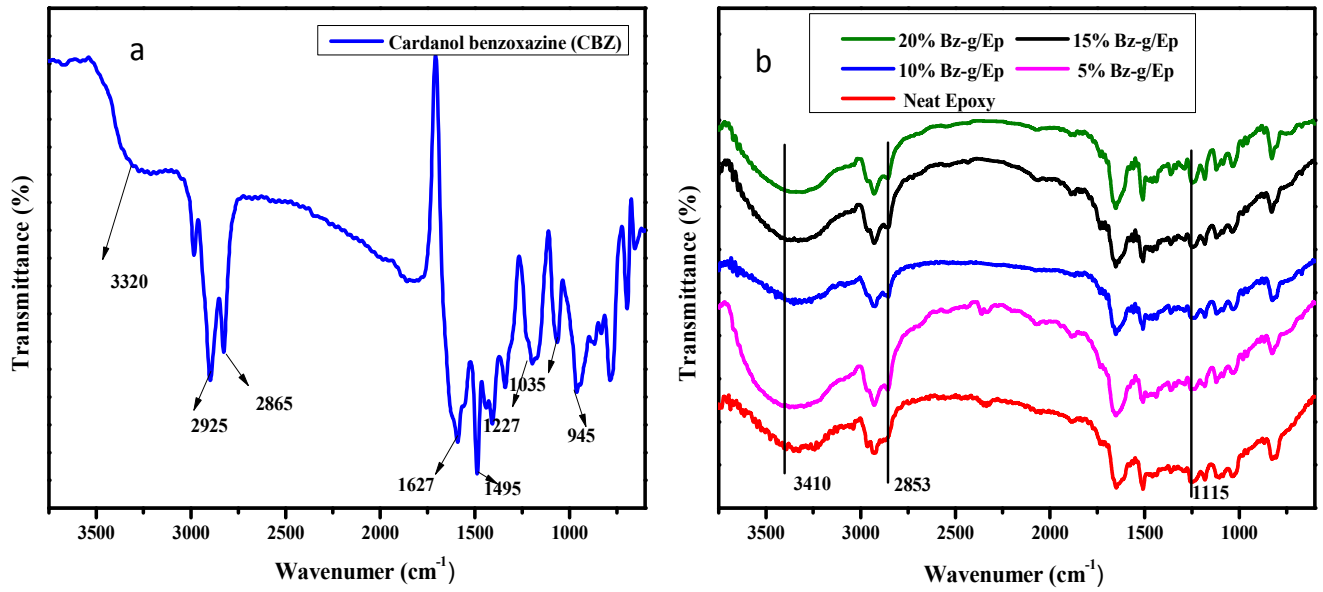

Figure 2. FTIR spectra of (a) Cardanol benzoxazine (b) Neat epoxy and Bz-g/Ep composites.

The peak appeared at 1495 cm^{-1} is due to the trisubstituted benzene ring of benzoxazine. The peak appeared at 1627 cm^{-1} represents C=C stretching vibration in benzene ring. Further the characteristic absorptions at 3320 cm^{-1} represents the functional hydroxyl group and the peaks appeared in ranges between 2925 and 2865 cm^{-1} corresponds to alkyl side chain of cardanol [23, 24].

Figure 2b illustrates the FT-IR spectra of the neat epoxy matrix and Bz-g/Ep nanocomposites. After thermal curing, the O^-. . ..H^+N intramolecular hydrogen bonding was observed around 2850 cm^{-1} and OH. . ..O intermolecular hydrogen bonding was observed around 3410 cm^{-1}.[25] The disappearance of peak at 946 cm^{-1} further confirms the formation of network structure. From 5wt% Bz-g/Ep to 20wt% Bz-g/Ep the characteristic absorption peaks again observed at 1115 cm^{-1} (symmetric stretching C-O-C) and 1258 cm^{-1} (asymmetric stretching C-O-C) are due to the formation of ether linkages in the Bz-g/Ep system. The intensity of absorption peaks at 1252 $cm^{-1}$and 1007 cm^{-1} is increased with increases of Bz-g/Ep content and this may be explained due to the formation of strong ether linkage between the hydroxyl groups of graphene and Polybenzoxazine.

NMR Spectra

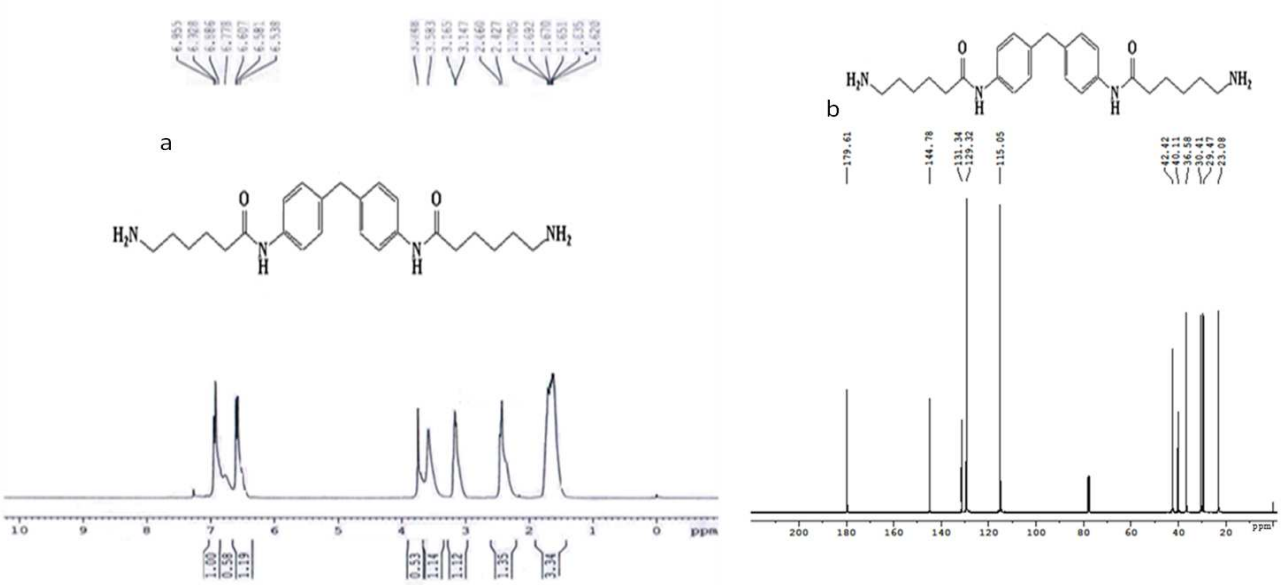

Figure 3. (a) ^{1}H NMR and (b) ^{13}C NMR spectra of CPA.

Figure 3a shows the ^{1}H NMR spectra of CPA, in the spectra aromatic protons appeared between 6.6 and 6.9 ppm, amine protons appeared between 3.1 and 3.5 ppm and the aliphatic protons appeared between 1.6 and 2.4 pm. In ^{13}C NMR (Figure 3b) the carbonyl carbons appeared at 179 ppm, aromatic carbons appeared between 115 and 144 ppm and aliphatic carbons appeared between 23 and 42 ppm.

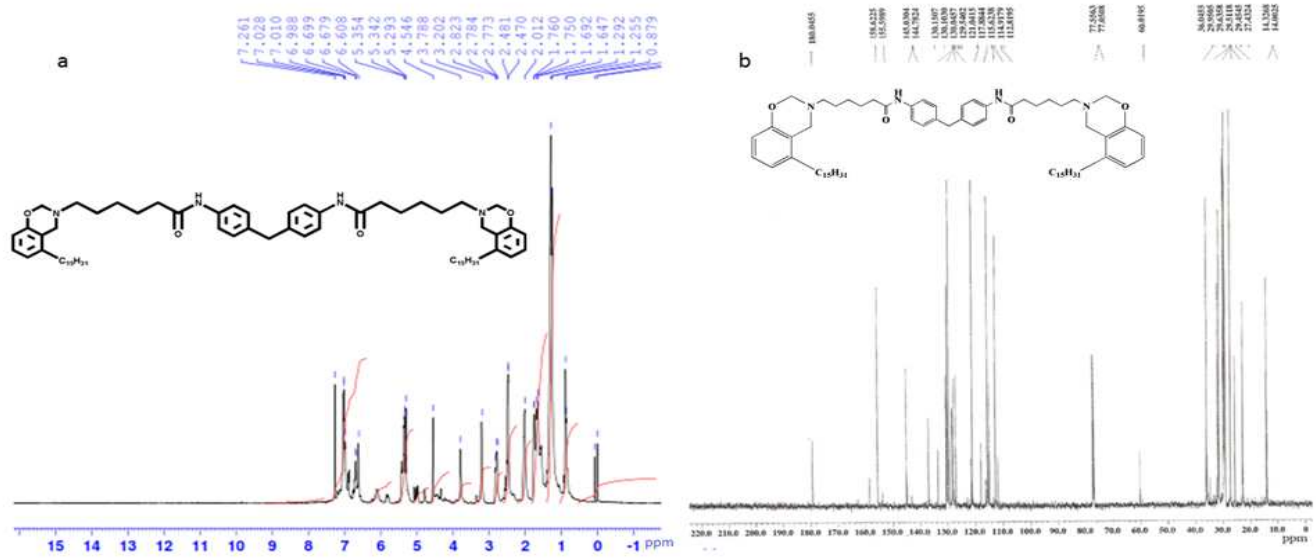

Figure 4. (a) ^{1}H NMR and (b) ^{13}C NMR spectra of CBZ.

Figure 4a shows the ^{1}H NMR spectra of cardanol benzoxazine (CBZ). From the spectra the peaks appeared from 6.75 ppm to 7.23 ppm were assigned to the aromatic protons. The characteristic protons of oxazine ring appeared at 4.5 ppm and 5.2 ppm are assigned to -O-CH2-N- and Ar- CH2-N- respectively. The amine protons appeared at 3.2 ppm and the peak at 5.36 ppm are due to the vinyl double bond C =CH protons of long alkyl side chain present in cardanol skeleton. In addition, all other aliphatic protons are appeared from 0.8ppm to 2.8 ppm. In ^{13}C NMR (Figure 4b) the carbonyl carbons appeared at 179 ppm, aromatic carbon appeared from 115 ppm to 144 ppm and aliphatic carbon atoms are appeared from14 ppm to 36 ppm [26].

XRD analysis

In the diffractogram (Figure 5a) of pristine graphite sample the peak appeared at 26.5^{0}, indicates the (002) plane with interlayer spacing of 0.34 nm, whereas (002) plane of the graphene appeared at 11.7^{0}, with increase in interlayer spacing of 0.75 nm. The shifting of (002) plane of graphite ascertains the formation of typical GO, and confirms the exfoliation of graphite during the oxidation process. The hybrid network structure of neat epoxy, 5wt% Bz-g/Ep, 10wt% Bz-g/Ep and 20wt% Bz-g/Ep nanocomposites were characterized with XRD and the data obtained are presented in Figure 5b. The XRD patterns exhibit a broad amorphous with peak maximum at 2θ = 18.5^{0} which implies that the graphene molecules are homogeneously dispersed in epoxy benzoxazine networks through covalent bonding in the hybrid nanocomposites.

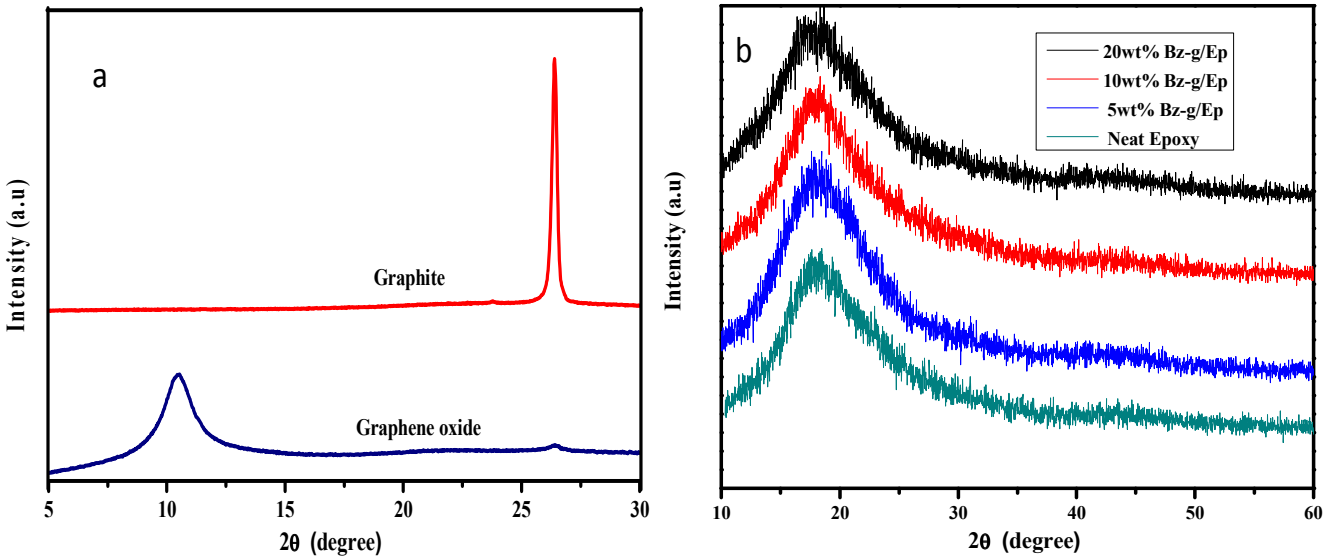

Figure 5. XRD spectra of (a) Graphene oxide and Graphene (b) Neat epoxy and Bz-g/Ep composites.

Raman Spectra

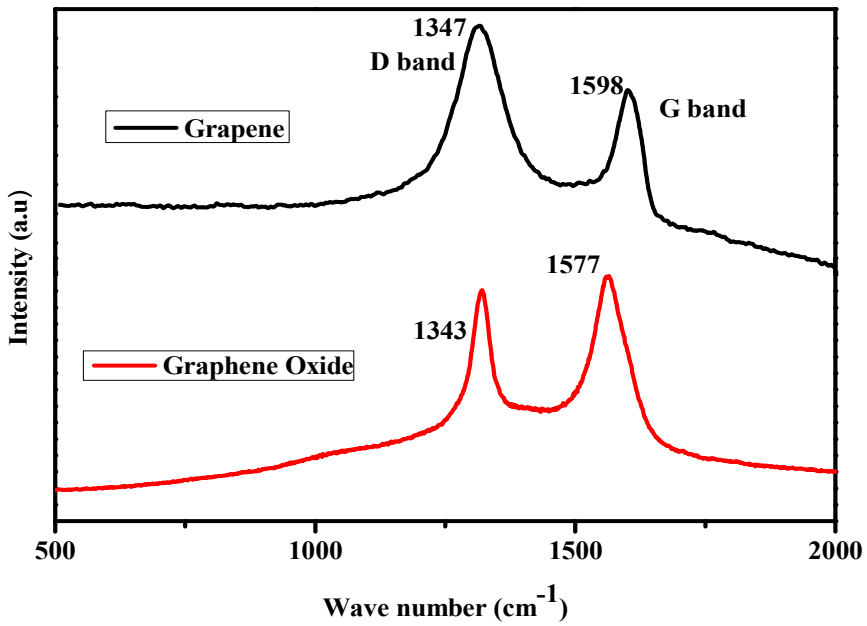

Figure 6. Raman spectra of graphene oxide and graphene.

Figure 6 represents the Raman spectra of graphene oxide and graphene. The G peak and 2D peak are the characteristics of sp2 hybridized carbon–carbon bonds in graphene. In graphene oxide, the D band appeared at 1343 cm^{-1} with lower intensity than that of the G band due to the decrease in the size of the sp2 plane. The G band appeared at 1573 cm^{-1} indicates the presence of isolated double bond resonances. After reduction of graphene oxide, the D and G bands of graphene are appeared at 1347 cm^{-1} and 1598 cm^{-1} respectively. (I_D/I_G) is an indicator for the disordered structure of the graphitic structure.The I_D/I_G value of graphene oxide is 0.89 after reduction of GO the value becomes 1.16. The increased I_D/I_G ratio of graphene after the chemical reduction of GO results modified structure of GO and this shows the occurrence of graphitisation in the reduced product[27,28].

Mechanical Properties

The mechanical properties of neat epoxy matrix, 5wt% Bz-g/Ep, 10wt% Bz-g/Ep, 15wt% Bz-g/Ep and 20wt% Bz-g/Ep are presented in Table 2. The impact strength of DGEBA matrix with 5wt% Bz-g/Ep, 10wt% Bz-g/Ep, 15wt% Bz-g/Ep and 20wt% Bz-g/Ep shows an improvement of 15%, 24%, 40% and 56% respectively when compared with that of neat epoxy matrix.

Table 2. Mechanical properties of neat epoxy and Bz-g/Ep nanocomposites

Sample Code	Tensile strength (MPa)	Flexural strength (MPa)	Impact strength (J/m)	Dielectric Constant (k)
Neat epoxy matrix	61.34	106.82	101.85	3.62
5wt% Bz-g/Ep	65.26	109.34	117.37	5.81
10wt% Bz-g/Ep	69.36	134.64	126.74	7.68
15wt% Bz-g/Ep	71.26	152.26	142.27	9.21
20wt% Bz-g/Ep	82.37	168.61	159.30	10.48

The improvement of impact strength is mainly attributed to the presence of flexible amide linkages (-NH-CO-) present in capron and the aliphatic skeleton of cardanol based benzoxazine [20, 29]. Thus the caprolactam based benzoxazine contributes to more flexibility to Bz-g/Ep composites. Thus the excess of free volume caused by the chain entanglement with high energy absorption is the key factor which contributes to the toughness behavior and the same was found more predominant in the case of capron based benzoxazine.

The values of flexural strength of 5wt% Bz-g/Ep, 10wt% Bz-g/Ep , 15% Bz-g/Ep and 20% Bz-g/Ep nanocomposites are increased to 2.3%, 26.04%,42.51% and 57.84%, respectively, when compared with that of neat epoxy matrix system. This is due to the formation of an interpenetrating network between the molecular chains of epoxy and caprolactam cardanol based benzoxazine and contributes an enhanced stress dissipating behaviour. The neat epoxy matrix shows the value of tensile strength of 61.34 MPa. Whereas the tensile strength values of 5wt% Bz-g/Ep, 10wt% Bz-g/Ep, 15wt% Bz-g/Ep and 20wt% Bz-g/Ep are 65.26, 69.36, 71.26 and 81.37 MPa respectively. The 20wt% Bz-g/Ep composite material shows the higher value of tensile strength than that of other composites, this infers that the highest interfacial interaction resulted between epoxy and Bz-g layers[30, 31]. In addition to interfacial interaction, the enhancement in the value of tensile strength is also due to the

intermolecular hydrogen bonding and long chain polar polyamide (PA6) and aliphatic skeleton in the benzoxazine, are these contributes to significant improvement in load bearing properties for the resulting composites.

Thermal stability of Bz-g/Ep nanocomposites

Thermo Gravimetric Analysis (TGA)

The thermal stability data obtained for neat epoxy matrix, polybenzoxazine (PCBZ) and Bz-g/Ep composites are shown in Figure 7 and Table 3. The neat epoxy matrix found to show an inferior thermal stability, whose char yield became zero at 550 ^{0}C, where as that of polybenzoxazine and Bz-g/Ep composites are increased to an appreciable extent. There is a small amount of weight loss below 240 ^{o}C in all the systems was noticed due to the removal of removal of water molecules, unreacted hydroxyl groups and carbonyl groups of acid from the graphene moiety of composites.

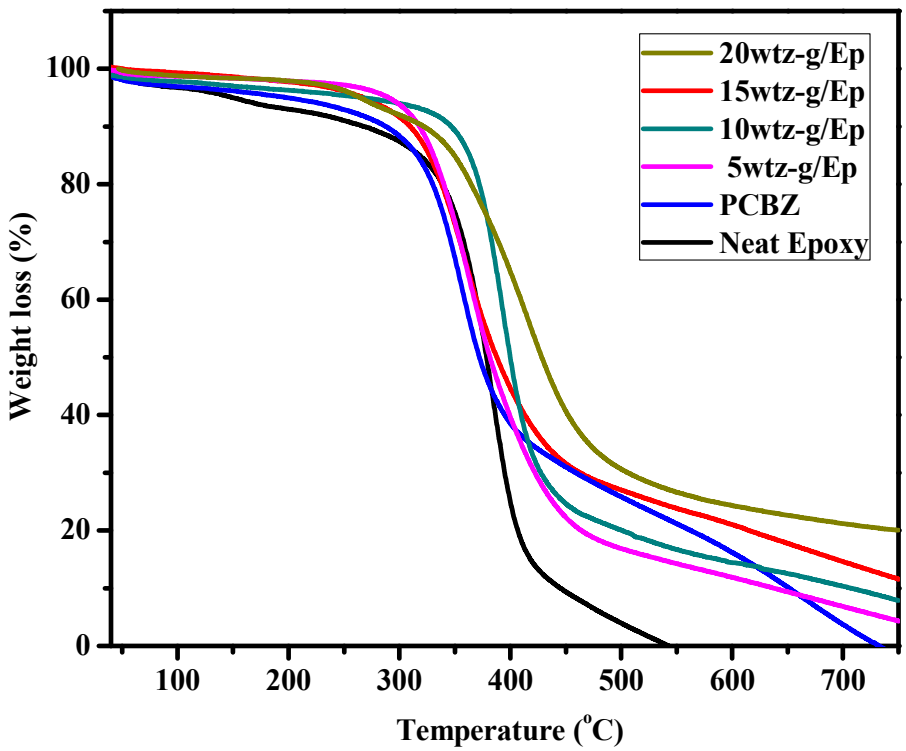

Figure 7. TGA profile of neat epoxy and Bz-g/Ep composites

However the degradation occurred between 320^{0}C to 430^{0}C was explained due to the decomposition of flexible amide segments of caprolactam of benzoxazine. The polybenzoxazine which contains flexible long chain with aromatic group degrades completely at 725^{0}C. Whereas, on increasing the wt% of benzoxazine-graphene in epoxy system the significant improvement in thermal stability was noticed. The char yield values of 5wt% Bz-g/Ep, 10wt% Bz-g/Ep, 15wt% Bz-g/Ep and 20wt% Bz-g/Ep are 4.5%, 8.0%, 11.6% and 19.8% respectively. This is due to the long aliphatic chain with aromatic moiety present in the cardanol which imparts more steric hindrance and further the reinforcement of graphene improves thermal stability with restricted the chain moility[32,33].

Table 3. Thermal properties of neat epoxy and Bz-g/Ep nanocomposites.

Sample Code	Weight loss			Char Yield at 750 (°C)	T_g (°C)
	20 (%)	40(%)	60 (%)		
	Temperature (°C)				
Neat epoxy	339	370	386	0	167
Polybenzoxazine(PCBZ)	330	358	394	0	-
5wt% Bz-g/Ep	340	367	400	4.5	183
10wt% Bz-g/Ep	372	391	410	8.0	189
15wt% Bz-g/Ep	338	370	413	11.6	199
20wt% Bz-g/Ep	364	410	452	19.8	210

Differential Scanning Calorimetry (DSC)

The DSC analyses of epoxy reinforced with different weight percentages of Bz-g/Ep composites are illustrated in Figure 8 and Table 3. From the Table it is observed that the neat epoxy matrix exhibits the value of glass transition temperature of 167 ^{0}C and the Tg value is increased with increase in weight percentages of Bz-g/Ep. This is due to the enhanced chain entanglement resulted between the graphene

reinforced benzoxazine and epoxy matrix as well as with polyamide and cardanol segment of benzoxazine. The Bz-g restricts the chain mobility of the matrix due to the inter flake interaction and pi-pi stacking between the graphene with epoxy and benzoxazine. The 20wt% Bz –g shows the highest value of Tg of 210 ^{0}C and is due to the enhanced crosslinking and entanglement of long molecular chains present in the network.

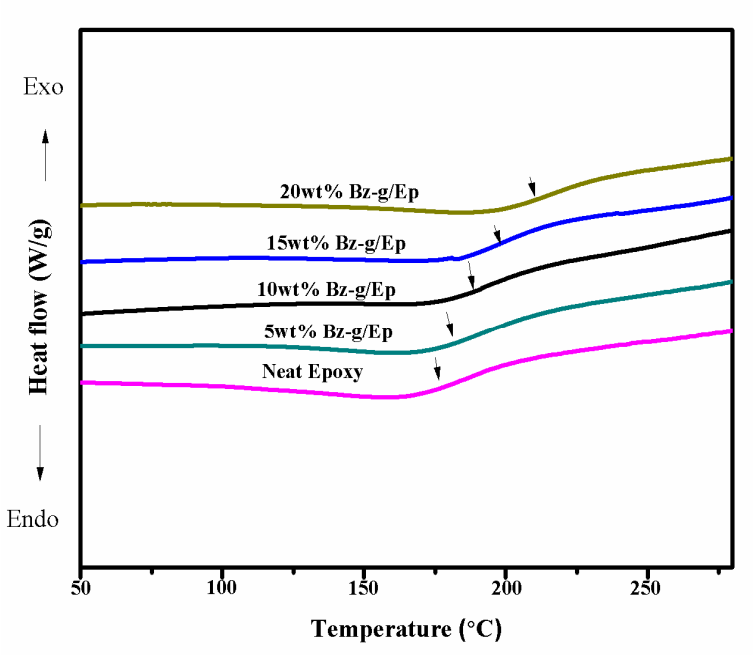

Figure 8. DSC profile of neat epoxy matrix and Bz-g/Ep composites.

Dielectric constant (k)

The value of dielectric constant of the neat epoxy matrix and Bz-g/Ep nanocomposites are presented in Figure 9a and Table 2. With the increasing wt% of Bz-g to epoxy, the value of dielectric constant was increased. The value of dielectric constant of neat epoxy matrix is 3.6 and is increased to 5.8 for 5wt % Bz-g/Ep at 1 MHZ and subsequently increased to 7.6, 9.2 and 10.5 with increasing concentration of Bz-g 10, 15 and 20wt% respectively. An incorporation of filler and/or reinforcement in polymer matrix influences the dielectric behaviour of the reinforcing composites. The reinforcing materials have a significant effect on the migration and accumulation of charge carriers at the interfaces. An improvement of average electric field of the polymer matrix, attained with the reinforcement of graphene contributes to the enhanced value of dielectric constant. The increase in the value of dielectric

constant was attributed to the motion of free charge carriers due to the formation of continuous conductive pathway throughout the nanocomposites [34].

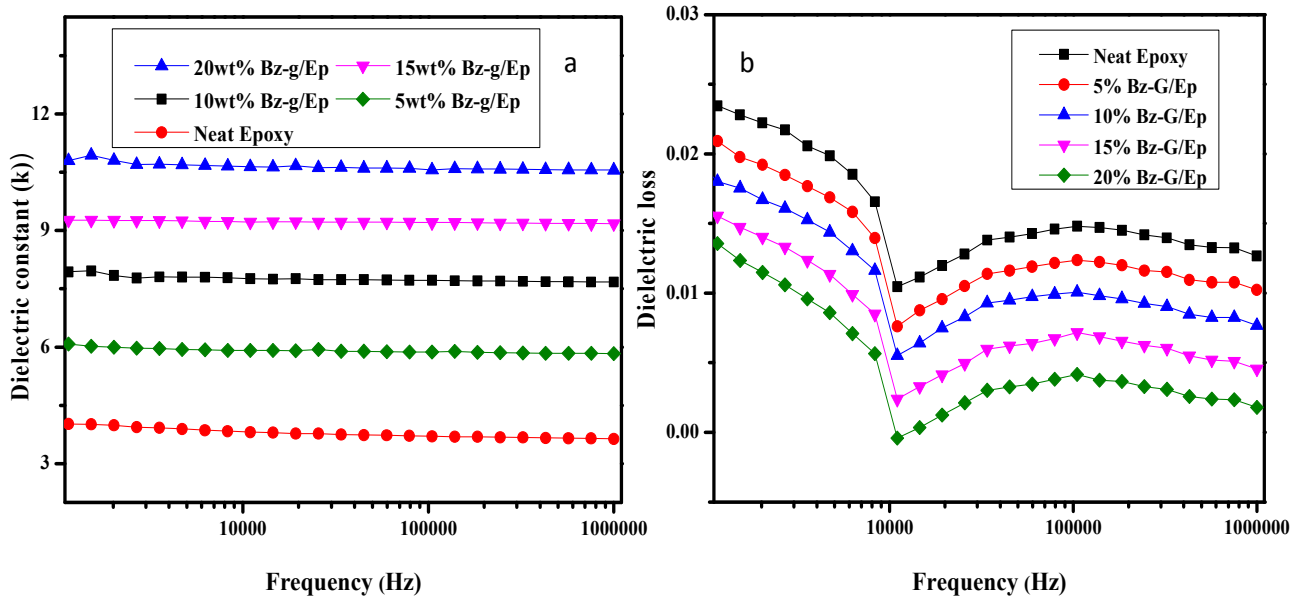

Figure 9. A plot of electrical properties dependent on frequency for neat epoxy matrix and Bz-g/Ep nanocomposites (a) Dielectric constant (b) Dielectric loss.

Homogeneous dispersion of graphene into the epoxy matrix creates a local amplified electric field and thus contributes to an enhanced value of capacitance to the nanocomposites. Hence, an increase in the value of dielectric constant was observed with an increase in wt % benzoxazine- graphene content, where as it was also found to be decreased with increase in frequency, which is attributed to the occurrence of leakage current from the long-range transport of charge carrier in the low frequency range[35].

The values of dielectric loss are presented in Figure 9b for neat epoxy and Bz-g/Ep nanocomposites. At 1 MHz the tan δ value for neat epoxy matrix is about 0.012, whereas in the case of 20wt% Bz-g/Ep shows the tan δ value is 0.001. It was observed that there was no appreciable change in the value of dielectric loss for 20wt% Bz-g-Ep at higher frequency range. Therefore, the lowering of dielectric loss tangent of a graphene reinforced benzoxazine/epoxy can be explained due to formation of insulating layer outer to the dielectric centre and thus results the restricted migration and accumulation of charges

within the nanocomposites. Data from dielectric studies infers that these materials can be used as an effective and efficient high k material for microelectronic applications.

Effect of Bz-g/Ep loading on Morphological Properties.

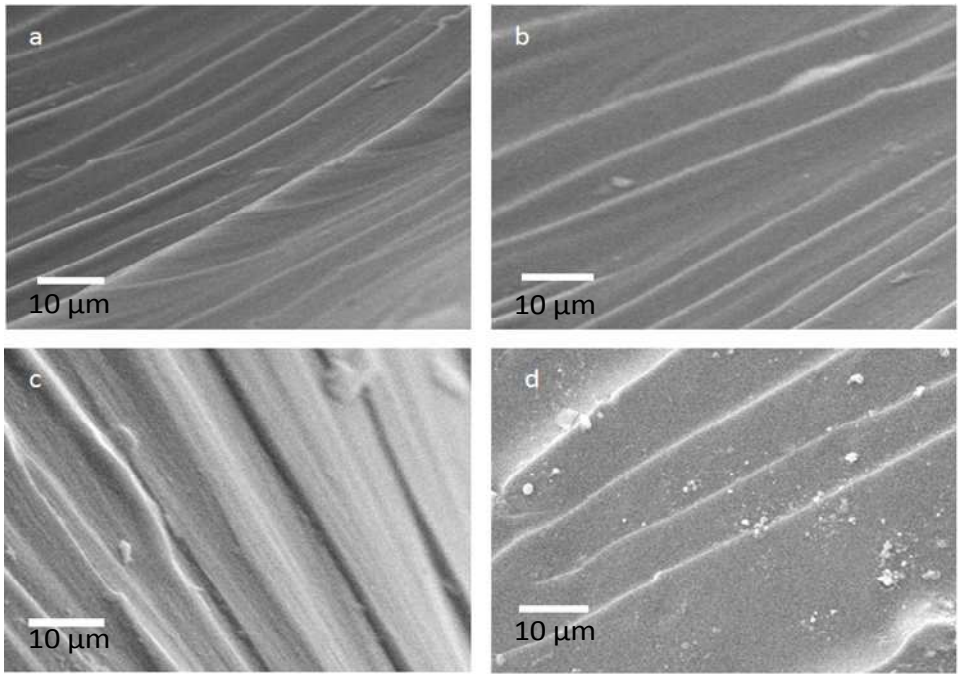

Figure 10. SEM images of (a) 5wt% Bz-g/Ep, (b) 10wt%s Bz-g/Ep, (c) 15wt% Bz-g/Ep and (d) 20wt% Bz-g/Ep composites.

Figure 10 illustrates the SEM images of fractured surfaces of 5wt% Bz-g/Ep, 10wt% Bz-g/Ep, **1**5wt% Bz-g/Ep and 20w**t**% Bz-g/Ep composites. From the images it is inferred that the graphene layers are well dispersed in the benzoxazine/epoxy matrix without any significant aggregation. The fractured surface of the sample shows higher amount of rough surface which might be due to the presence of graphene in the polymer composite. It is clearly ascertained that with an increase in Bz-g wt%, there was the formation of small clusters due to polyamide linkage of benzoxazine and were found in the epoxy matrix at lower level of reinforcement. Thus the nanocomposites hold two phases such as nanofibril phase and normal matrix phase and these results are concur with the literature reported[36].

Transmission Electron Microscope (TEM)

TEM images of 20% Bz-g/Ep nanocomposites are presented in Figure 11. The presence of graphene layer in the epoxy/benzoxazine network is clearly seen in Figure 11(a and b). These results indicate that the Bz-g/Ep nanocomposites possess good interfacial interaction through the chemical bonding. The nanometer-level dispersion of the graphene molecules in the epoxy matrix influences the thermal and electrical properties of the composites.

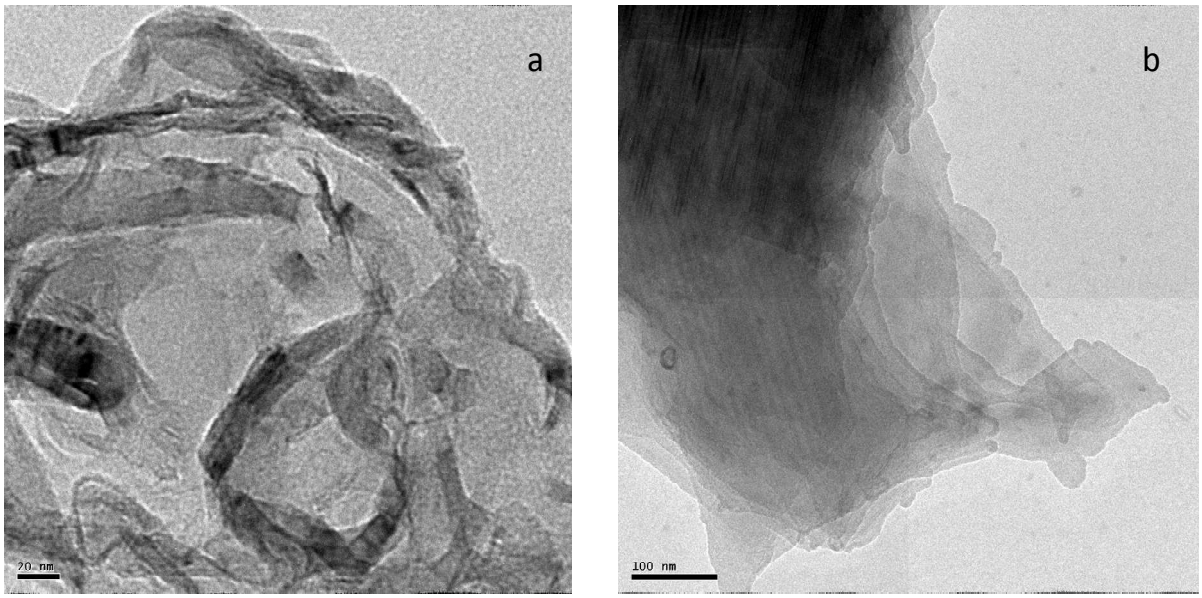

Figure11. TEM image of 20% Bz-g/Ep composites.

Surface free energy

The contact angle measurements were performed using a goniometer and the values are presented in Figure 12 and Table 4. The values of contact angle of neat epoxy matrix and different weight percentages (5,10,15 and 20 wt%) of Bz-g/Ep reinforced composites are 75.6°, 78.4°, 80.2°, 84.7° and 90.0 respectively using 5 µl of deionised water as probe liquid, which infers that the hydrophobic nature increased with increase in wt% of benzoxazine. Similarly when diiodomethane was used as a dispersive liquid the value of contact angle was found to be 40.5°, 48.3°, 56.1°, 57.6° and 60.3^{o} respectively.

Table 4. The values of contact angle and surface free energy of neat epoxy matrix and Bz-g /Ep composites.

Sample Code	Contact angle (^{0})		Surface free energy (J/m^{-1})		
	Water	DI	Υ^d	Υ^p	Γ
Neat epoxy	75.6	40.5	39.4	6.4	45.8
5% Bz-g/Ep	78.4	48.3	35.2	5.2	40.4
10% Bz-g/Ep	80.2	57.6	33.9	2.6	36.5
15% Bz-g/Ep	84.7	50.5	32.2	1.9	34.1
20% Bz-g/Ep	90.0	60.3	30.5	1.2	31.7

The value of contact angle can be used to estimate the surface free energy of composites surfaces. The surface free energy (Γ) of neat epoxy matrix and Bz-g/Ep nanocomposites were calculated according to the geometric mean model[37].

$$\text{Cos}\theta = 2/\gamma_L \left[(\gamma_L^d \gamma_s^d)^{1/2} + (\gamma_L^p \gamma_s^p)^{1/2}\right] \quad (1)$$

$$\gamma_s = \gamma_s^d + \gamma_s^p \quad (2)$$

Where θ is the contact angle and γ_L is the liquid surface tension; and γ_s^d and γ_s^p are the dispersive and polar components of γ_L, respectively

From Table 4, it can be seen that the 20% Bz-g/Ep nanocomposites exhibited the lowest value of surface free energy (31.7 mJ/m^2) when compared to that of other percentages of Bz-g reinforced nanocomposites. This is attributed due to the effective interaction occurred between benzoxazine and the epoxy matrix, which favors the enhanced hydrophobic behaviour of the resulted matrix.

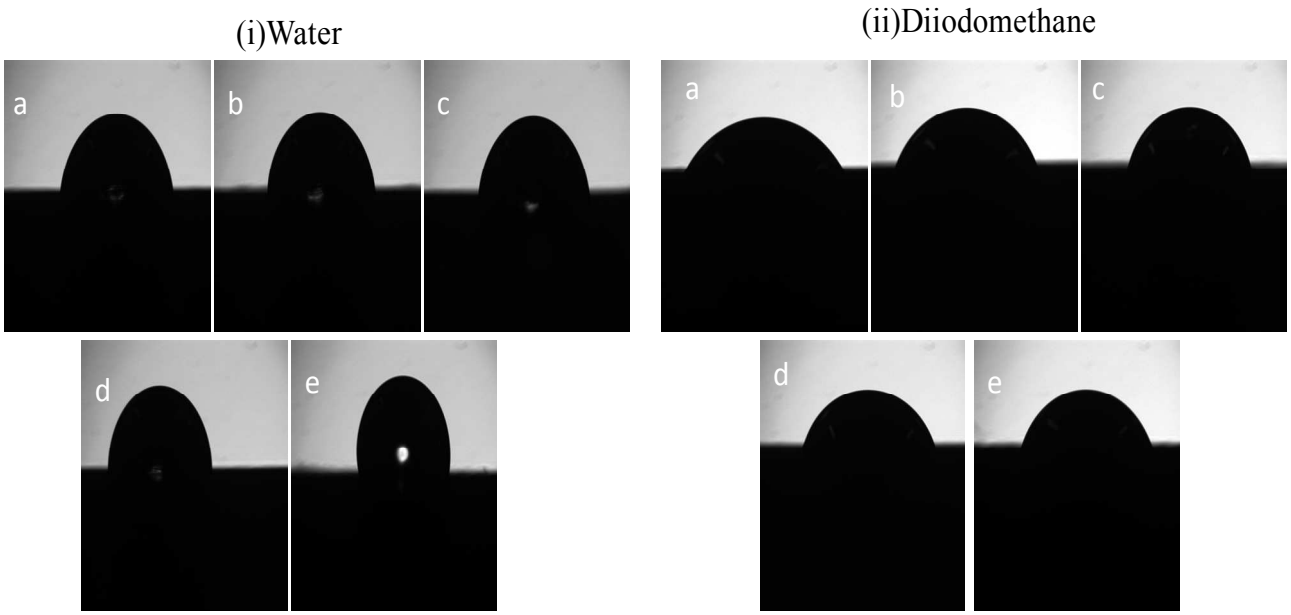

Figure 12. Contact angle images of (a) Neat epoxy matrix (b) 5%Bz-g/Ep,(c) 10%Bz-g/Ep,(d) 15%Bz-g/Ep and (e) 20%Bz-g/Ep composites.(i) Water (a-e) and (ii) Diiodomethane(a-e).

Conclusion

Epoxy based toughened nanocomposites have been prepared by casting technique, with varying weight percentages of Bz-g. Data obtained from thermo-mechanical and dielectric properties show that 20% Bz-g/Ep possess improved properties than those of neat epoxy matrix and other weight percentages of Bz-g/Ep reinforced composites. The contact angle studies show that 20% Bz-g/Ep possesses the lowest surface free energy than that of other samples. TEM analysis further supports the homogeneous dispersion of graphene to benzoxazine/epoxy composites. Data obtained from different studies indicate that, these materials can be used in the form of coatings, adhesives, sealants, encapsulants etc., as dielectric materials in microelectronic applications for better performance with improved longevity.

Acknowledgment

The authors thank CSIR G. No: 02(0112)/12/EMR-II CSIR, New Delhi , Govt. of India., for the financial support and also thank to Dr. M.R.Vengatesan, South Korea, Dr. S. Devaraju, Pusan National

University, Busan, R.Sasi Kumar and Mrs. Kanimozhi, Research Scholar Dept. of Chemical Engineering, AC Tech, Anna University for their support.

References

1. Y. Yagci, B. Kiskan and N.N. Ghosh, J Polym Sci Part A: Polym Chem, 2009, **47**, 5565.
2. N.N. Ghosh, B. Kiskhan, and Y. Yagci, Prog. Polym. Sci., 2007, **32**, 1344.
3. C.P. Reghunadhan Nair, Prog. Polym. Sci., 2004, **29**, 401.
4. A. Chernykh, T. Agag and H. Ishida, Polymer, 2009, **50**, 382.
5. Y. Liu, S. Zhao, H. Zhang, M. Wang, and M. Run, Thermochim.Acta, 2012, **42**, 549.
6. C. Andronescu, S.A. Garea, C. Deleanu, and H. Iovu, Thermochim.Acta, 2012, **4**, 530.
7. H. Ishida and D.J. Allen, Polymer, 1996, **35**, 4487.
8. D.D.L. Chung, Polym. Polym. Compos. 2000, **8**, 219.
9. Z.M. Dang, J. K. Yuan, J.W. Zha, T. Zhou, S.T. Li and G.H. Hud, Prog. Mater Sci., 2012, **57**, 660.
10. K. S. Novoselov, A. K. Geim, S. V. Morozov, D. Jiang, Y. Zhang, S. V. Dubonos, I. V. Grigorieva and A. A. Firsov, Science, 2004, **306**, 666.
11. L.M. Veca, M. J. Meziani,W. Wang, X. Wang, F. S. Lu, P. Y. Zhang, Y. Lin, R. Fee, J. W. Connell and Y. P. Sun, Adv. Mater., 2009, **21**, 2088.
12. V. E. Muradyan, A. A. Arbuzov, E. A. Sokolov, S. D. Babenko, and G. V. Bondarenko, Tech Phys Lett., 2013, **39**, 1.
13. L.C. Tang,Y. J.Wan, K. Peng, Y.B. Pei, L.B. Wu and L.M. Chen, Compos Part A, 2013, **45**, 95.
14. S. Nagendiran, M. Alagar and I. Hamerton, Acta Materialia, 2010, **58**, 3345.
15. M.R. Vengatesan, S. Devaraju and M. Alagar, High performance Polymers, 2011,**23**,3.
16. S. Nagendiran, S. Premkumar and M. Alagar, Journal of Applied Polymer Science 2007,**106**, 1263.
17. R. Verdejo, M.M. Bernal, L.J. Romasanta and M.A. Lopez-Manchado, J Mater Chem 2011, **21**, 3301.
18. K. Huanga, Y. Zhanga, L. i. Mei, J. Lian, Y. Xiaohua and X. Jianling, Progress in Organic Coatings, 2012, **74**, 240.
19. S. Sahila, L.S. Jayakumari, Polymer Composites, 2014, DOI 10.1002/pc
20. K.Sethuraman, P. Prabunathan and M. Alagar, RSC Advances, 2014, **4**, 45433.
21. X.F. Zhou and Z.P. Liu, Chem. Commun. 2010, **46**, 2611.

22. K. Sethuraman, P. Prabunathan and M. Alagar, RSC Advances, 2014, **4**, 30485.

23. T. Agag and T. Takeichi, Macromolecules, 2003, **36**, 6017.

24. Y.J. Lee, J.M. Huan, S.W. Kuo, J. K. Chen and F.C Chang, Polymer, 2005,**46**, 2320.

25. J. Wang, X. Fang, M.Q. Wu, X. Y. He, W.B. Liu, and X. D. Shen, Eur. Polym. J. 2011, **47**, 2158

26. B.S. Rao and Aruna Palanisamy, Progress in Organic Coatings, 2012, **74**, 427.

27. S. Stankovich, D. A. Dikin, R. D. Piner, K. A. Kohlhaas, A. Kleinhammes, Y. Jia, Y. Wu, S. T. Nguyen and R. S. Ruoff, Carbon, 2007, **45**, 1558.

28. V. C. Tung, M. J. Allen, Y. Yang and R. B. Kaner, Nat. Nanotechnol., 2008, **4**, 25.

29. S. Premkumar, C. K. Chozhan and M. Alagar, Eur. Polym. J., 2008, **44**, 2599.

30. L.C. Tang a, Y.J. Wan, D. Yan, Y.B. Pei, L. Z, Y.B. Li, L.B. Wu, J.X. Jiang and G.Q. Lai, Carbon, 2013, **60**, 16.

31. Y.J. Wan, L.C. Tang, L.X. Gong, D. Yan, Y.B. Li, L.B. Wu, J.X. Jiang and G.Q. Lai, Carbon, 2014, **69**,467.

32. M. Selvi, S. Devaraju, M. R. Vengatesan, J. S. Go, Manmohan Kumar and M. Alagar, RSC Advances, 2014, **4**, and 8238.

33. W. Gao, L. B. Alemany, L. Ci and P. M. Ajayan, Nat. Chem., 2009, **1**, 403.

34. Y. Zhang, Y. Wang, Y. Deng, M. Li, and J. Bai, Mater. Lett., 2012, **9** 72.

35. N. J. Delollis and O. Montoya, J. Appl. Polym. Sci., 1967, **11**, 983.

36. S. Ahmadi, J. Morshedian, S.A. Hashemi, P.J. Carreau, and W. Leelapornpisit, Iran Polym J., 2010, **19**, 229.

37. S. Devaraju, M. R. Vengatesan, M. Selvi, A. Ashok Kumar, I. Hamerton, J. S. Go and M. Alagar, RSC Adv., 2013, **3**, 12915.